Unlocking Blue Carbon's Potential Requires Targeted Uncertainty Reductions

Shawn Doyle[1], Hoonshin Jung[1,2*], and Tim Carruthers[3]

[1] The Water Institute, Baton Rouge, LA, USA.
[2]U.S. Army Corps of Engineers, New Orleans, LA, USA.
[3]South Australian Government, Adelaide, South Australia, Australia.
E-mail: sdoyle@thewaterinstitute.org; Hoonshin.Jung@usace.army.mil; tim.carruthers@sa.gov.au

Keywords: Blue Carbon, Sensitivity Analysis, Coastal Wetlands, Carbon Crediting

Note: This is a non-peer reviewed preprint submitted to EarthArXiv

ABSTRACT

Coastal "blue" carbon ecosystems like swamps and marshes are among the most efficient natural carbon sinks on Earth. Consequently, restoring and conserving these wetlands is gaining interest from private and government stakeholders as a nature-based solution to offset greenhouse gas emissions and generate revenue through carbon credits. However, the financial viability of blue carbon crediting is currently challenged by major uncertainties in quantifying net greenhouse gas fluxes from these dynamic systems. To better understand the drivers of this uncertainty, we conducted a sensitivity analysis to identify the most influential parameters affecting net carbon flux estimates over 30 years. Our analysis examined parameters from sub-basin (~60,000 ha) to the coastal ecosystem (~3,000,000 ha) scale, considering parameters such as the fate of soil carbon from marsh erosion, methane and nitrous oxide emissions, and changes in plant productivity. We found that the relative importance of these parameters varied by wetland type as well as the spatial and temporal scale of analysis. This confirmed that applying broad assumptions or default values in carbon flux calculations result in highly uncertain estimates, which can often vary by over 100%. In fresh and intermediate salinity wetlands, carbon flux estimates were most sensitive to the high uncertainty in methane and nitrous oxide emission rates. In contrast, brackish and saline wetlands showed greater sensitivity to variability in annual plant growth. However, where wetlands were prone to erosion, the fate of eroded soil carbon stores became the dominant source of uncertainty in net carbon flux estimates, particularly over longer (20+ years) time scales. By identifying which parameters contribute most to uncertainty in coastal carbon flux estimates at different spatial and temporal scales, our study helps target research and monitoring efforts towards those that can provide the greatest reduction in uncertainty, moving blue carbon crediting projects towards financial viability.

INTRODUCTION

"Blue carbon" refers to greenhouse gases, such as carbon dioxide (CO_2), methane (CH_4), and nitrous oxide (N_2O), that are captured, sequestered, or emitted by vegetated coastal and marine ecosystems such as tidal forested wetlands, salt marshes, mangrove swamps, and seagrass meadows—

hereafter referred to as blue carbon ecosystems. Compared to “green carbon” ecosystems like forests—which store most of their carbon in aboveground biomass—blue carbon ecosystems store up to 95% of their carbon in their soils (Alongi, 2020), which are often water-saturated and anoxic. The lack of oxygen in these soils slows microbial decomposition processes and causes organic matter to accumulate over time (Macreadie et al., 2017). As a result, carbon sequestered in blue carbon ecosystems can remain stored for millennia, making these ecosystems among the most efficient natural carbon sinks on Earth (Belshe et al., 2019; Kelleway et al., 2017; Lovelock & Reef, 2020; Macreadie et al., 2019, 2021; Wylie et al., 2016). Globally, blue carbon ecosystems store an estimated 84–234 Tg of carbon per year, and on a per area basis sequester between 10× and 50× more than boreal, temperate, and tropical forests (Mcleod et al., 2011; Wylie et al., 2016). However, quantifying this storage accurately over time is challenging as these coastal tidal wetlands are highly dynamic at annual, decadal, and century timescales.

Blue carbon ecosystems have an important role to play in climate change mitigation (Macreadie et al., 2019, 2021; Rosentreter et al., 2023), but are highly threatened and are degraded or destroyed at a rate four times greater than that of tropical forests (da Silva Copertino, 2011). Major threats include mangrove deforestation, coastal and urban development, watershed pollution, eutrophication, sea level rise, local subsidence, edge erosion, and major storm events.

Due to these threats to blue carbon ecosystems and their ability to sequester and store carbon far more efficiently than other ecosystems, efforts to restore and conserve them using carbon financing mechanisms have begun to attract substantial interest from commercial and government stakeholders as a nature-based solution to offset greenhouse gas emissions (Friess et al., 2022; Wylie et al., 2016). Restoring and conserving these ecosystems alone may represent up to 14% of global natured-based mitigation opportunities needed to hold warming to <2 °C (Griscom et al., 2017). Despite this interest, the commercial viability of blue carbon offset crediting is currently limited by challenges in forecasting the climate mitigation benefit of a blue carbon project over its lifespan with reasonable confidence (Williamson & Gattuso, 2022). These challenges are largely driven by uncertainties surrounding various parameters, ranging from natural variability in aboveground net primary productivity (ANPP) and CH_4 and N_2O fluxes across habitat types to accounting for the consequences of coastal erosion and the subsequent potential loss of previously stored soil carbon stocks (Alongi, 2012; Carruthers et al., 2024; Mcleod et al., 2011; Spivak et al., 2019).

In this study, we used extended Fourier amplitude sensitivity tests (eFAST; (Saltelli et al., 1999)) to systematically evaluate the relative importance of uncertainties in blue carbon flux estimates across Louisiana's coastal salinity gradient, encompassing both vegetated and open water habitats. Our multi-scale analysis quantified how variations in input parameters influenced net CO_2 equivalent (CO_2e) flux estimates at three distinct levels: locally at Port Fourchon, across the Barataria Basin watershed, and regionally throughout coastal Louisiana. Through this comprehensive approach, we aimed to identify critical knowledge gaps where targeted research could most effectively reduce uncertainty in carbon flux quantification within these blue carbon ecosystems, thereby improving the financial viability of carbon offset crediting projects in coastal areas.

MATERIALS AND METHODS

STUDY AREA

Coastal Louisiana, USA, was used to identify the primary drivers of uncertainty in net carbon flux from sub-basin to coastal ecosystem scale: (1) Port Fourchon, (2) Barataria Basin, and (3) coastal Louisiana (**Figure 1**). Port Fourchon is surrounded by tidal wetlands including brackish marsh (dominated by saltmeadow cordgrass; *Spartina patens*), saline marsh (dominated by smooth cordgrass; *Spartina alterniflora*), mangrove forest (dominated by black mangrove; *Avicennia germinans*), and saline open water (salinity > 15 ppt). Port Fourchon, Barataria Basin, and coastal Louisiana are all experiencing significant tidal wetland loss due to compounding effects of local subsidence, eustatic sea level rise, and limited sediment supply (Dietz et al., 2018). This dynamic landscape makes these areas valuable for assessing how the uncertainties surrounding blue carbon dynamics impact tidal wetland carbon fluxes at different spatial scales under conditions of high land loss.

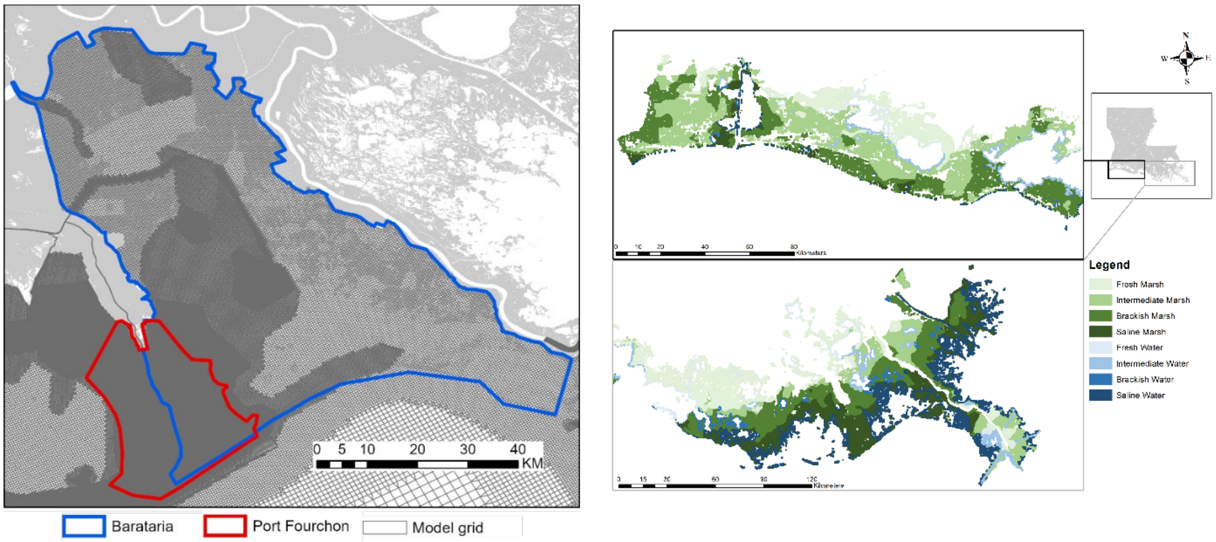

Figure 1. *(Left) Map of flexible mesh grid for modeling net carbon fluxes across Port Fourchon and Barataria Basin. The red border denotes the model run area for Port Fourchon, LA, the small-scale study area. The blue border denotes the model run area for Barataria Basin, LA, the basin-scale study area. (Right) Map of the area of coastal Louisiana modeled for the regional-scale analysis.*

NET CARBON FLUX CALCULATIONS

Changes in the landscape and habitats under future environmental conditions were predicted using an ensemble of hydrodynamic, morphology, and vegetation distribution models. Coupled hydrodynamic, wave, and morphodynamic models were developed using the Delft3D FM modeling suite (Deltares, 2019) to predict land and water bottom elevations based on interactions with tide, wave, and meteorological events (e.g., cold fronts, storms, etc.). The hydrodynamic model was calibrated using field measurements from 2015 and 2016, including water elevation, flow velocity, waves, and salinity. Using the calibrated Delft3D FM models, a 30-year simulation was conducted (from 2020 to 2050) to predict landscape changes in the study areas using the Intermediate Regionally Adjusted future environmental scenario described in Louisiana's 2023 Coastal Master Plan (White et al., 2023) Relative sea level rise rate was assumed to be 0.25 m by 2050 based on Scenario S07-RCP 4.5 (NOAA GFDL, 2013). Spatially varying subsidence rates were derived from the deep subsidence values from Louisiana's 2023 Coastal Master Plan (Fitzpatrick et al., 2021), and wetland areas were allowed to vertically accrete to keep up with relative sea-level rise (RSLR; Herbert et al., 2021; Kirwan et al., 2016). A 30-year series of synthetic tropical storms, quiescent weather conditions, and winter front events were also modeled (Johnson &

Geldner, 2020). In the case of storms, 27 predefined storms over a 30-year period were sequentially applied during the summer months within this framework.

Physical outputs (salinity, temperature, water depth, etc.) from the Delft3D FM coastal hydrodynamic, morphology, and wave models were used as inputs to a modified version of the LAVegMod.v2 wetland vegetation species distribution model (Visser & Duke-Sylvester, 2017). This modified vegetation distribution model (LAVegMod.PF) also predicts the distribution of black mangroves, uses annual mean salinity and water level variation to determine plant species distribution, incorporates an adaptive procedure that maintains open water coverage in existing wetlands, converts open water to bare ground in marsh creation areas, and limits vegetation mortality and establishment functions to the vegetated portions of grid cells. LAVegMod.PF was used to predict the percent coverage of 13 habitat types across a flexible mesh grid placed over the project areas (**Figure 1**) from 2020 to 2050.

Additional modifications to net carbon flux calculations across the modeled areas include updated ANPP values for each habitat type based on new field measurements (Supplemental Material). This included updated ANPP estimates for mangroves that now account for mangrove forest age: Young mangrove forests were defined as newly established mangrove areas (≤ 1 year), intermediate mangrove forests were defined as between 1 and 5 years old, and mature mangrove forests were defined as being over 5 years.

Once vegetation types and percent cover are estimated from LAVegMod.PF for the grid cells, a post-processing module was used to calculate net carbon flux across the modeled areas. The module uses a habitat carbon flux lookup table (**Table 1**) to estimate rates of ANPP and non-CO_2 greenhouse gas (i.e., $CH_4 + N_2O$) emissions (GHG) from each grid cell. Primary data sources for this lookup table are detailed in **Table S1** and **Table S2**. Soil carbon accumulation (SCA) rates for land habitats were modeled for each grid cell using the linear regression approach described in Herbert et al. (2021) that considers the effect of

RSLR on wetland soil carbon accumulation (Eq. 1). For open water areas, SCA rates (**Table 1**) were instead derived from averages of literature-derived values (Hillmann et al., 2020; Smith et al., 1983).

$$\text{mean SCA } (\text{g C m}^{-2}\text{ yr}^{-1}) = 52.61 \times 24.78 \times \text{RSLR } (\text{mm yr}^{-1}) \quad (1)$$

Table 1. *ANPP, SCA, and GHG rates (± sd) for each habitat type. All values are tons of CO_2e ha^{-1} yr^{-1}*

Habitat	**ANPP**	**SCA**	**GHG**
Fresh forested wetland	-16.06 ± 7.28	modeled from RSLR	24.58 ± 24.07
Freshwater marsh	-23.66 ± 11.65	modeled from RSLR	29.62 ± 33.58
Intermediate marsh	-24.10 ± 7.30	modeled from RSLR	29.62 ± 33.58
Brackish marsh	-47.31 ± 24.22	modeled from RSLR	5.86 ± 6.32
Saline marsh	-33.63 ± 15.85	modeled from RSLR	3.77 ± 9.31
Young mangrove forest	-33.80 ± 12.5	modeled from RSLR	9.56 ± 19.96
Intermediate mangrove forest	-71.70 ± 26.5	modeled from RSLR	9.56 ± 19.96
Mature mangrove forest	-85.95 ± 31.8	modeled from RSLR	9.56 ± 19.96
Fresh open water	-1.42 ± 1.65	-5.2 ± 1.8	0.28 ± 0.25
Intermediate open water	-1.42 ± 1.65	-5.2 ± 1.8	0.28 ± 0.25
brackish open water	-1.42 ± 1.65	-8.0 ± 0.7	0.15 ± 0.12
saline open water	-1.42 ± 1.65	-8.0 ± 0.7	0.03 ± 0.03
Bareground	0 ± 0	0 ± 0	0 ± 0

The annual net carbon flux for each grid cell, assuming no habitat changes, was then calculated using Eq. (2):

$$\text{Net carbon flux}_{\text{baseline}} = \sum\left(\left(\text{ANPP}_i + \text{SCA}_\text{i} + \text{GHG}_\text{i}\right)\right) \times \text{area}_\text{i} \quad (2)$$

where $\mathbf{ANPP}$, $\mathbf{SCA}$ and $\mathbf{GHG}$ (CH_4 + N_2O) are estimated annual fluxes in tonnes CO_2e ha^{-1} yr^{-1}, and $\mathbf{area_i}$ is the coverage (ha) within the grid cell for a given year. The final step to calculate net carbon flux for each grid cell was to account for carbon emissions resulting from the decay of aboveground (AG) biomass and/or the loss of stored belowground (BG) soil carbon that can occur after emergent wetland habitat conversion to open water (i.e., salt marsh erosion to open water) or habitat degradation (e.g., mangrove deforestation). These adjustments were performed using a modification of the approach described in Baustian et al. (2023), described here in Eqs. 3–7. Note, the *dT* term in Eqs. 5–7 allows for the annualization of CO_2 emissions from AG biomass and BG soil carbon decay that may occur after land loss, assuming a linear emission over the entire modeled time period.

$$\text{Net carbon flux} = \text{Net carbon flux}_{\text{baseline}} - \text{AG Biomass Decay} - \text{BG Soil Carbon Decay} \tag{3}$$

$$\text{AG Biomass Decay} = \text{Decay of woody vegetation} + \text{Decay of herbaceous vegetation} \tag{4}$$

$$\text{Decay of woody vegetation} = \sum\left(\text{WVD\%} \times \frac{\text{ANPP}_{\text{w}} \times \text{deforested}_{\text{w}}}{\text{dT}}\right) \tag{5}$$

$$\text{Decay of herbaceous vegetation} = \sum\left(\text{HVD\%} \times \frac{\text{ANPP}_{\text{h}} \times \text{degraded}_{\text{h}}}{\text{dT}}\right) \tag{6}$$

$$\text{BG Soil carbon decay} = \sum\left(\text{SCD\%} \times \frac{(\text{SCA}_{\text{i}} \times \text{converted}_{\text{i}} \times \text{soil carbon density})}{\text{dT}}\right) \tag{7}$$

Complete descriptions for each parameter are detailed in Table 2. For all parameters, a negative value indicates a carbon sink while a positive value indicates a carbon source.

Table 2. *Summary of algebraic terms used in net carbon flux calculations.*

Symbol	Description
$ANPP_i$	Aboveground net primary productivity rate (t CO_2e ha^{-1} yr^{-1}) for habitat i.
SCA_i	Annual soil carbon accumulation rate (t CO_2e ha^{-1} yr^{-1}) for habitat i.
GHG_i	Annual non-CO_2 greenhouse gas flux (t CO_2e ha^{-1} yr^{-1}) for habitat i.
$area_i$	Areal coverage of habitat type in hectares (ha) for habitat i.
i	Habitat type (e.g. brackish marsh, young mangrove forest, saline open water, etc.).
WVD%	Percentage (%) of <u>w</u>oody <u>v</u>egetation that <u>d</u>ecays after a woody habitat is deforested and converts to a marsh or open water.
HVD%	Percentage (%) of <u>h</u>erbaceous <u>v</u>egetation that <u>d</u>ecays after a marsh degrades and converts to open water.
SCD%	Percentage of a habitat's previously sequestered <u>s</u>oil <u>c</u>arbon that <u>d</u>ecays to atmospheric CO_2 after the habitat converts to open water.
$ANPP_w$	The ANPP within woody habitat types during the preceeding time period in which deforestation occurred. w = fresh forested wetland and mangrove forests.
$ANPP_h$	ANPP within herbaceous habitat types during the preceeding time period in which marsh degradation occurred. h = fresh, intermediate, brackish, and saline marshes.
$deforested_w$	Area (ha) of woody habitat types that were deforested and converted to marsh or open water during the preceeding time period. w = fresh forested wetland and mangrove forests.

$degraded_h$	Area (ha) of herbaceous wetlands that degraded to open water during the preceeding time period. h = fresh, intermediate, brackish, and saline marshes.
SCA_i	Annual soil carbon accumulation rate (t CO_2e ha^{-1} yr^{-1}) for habitat i during the preceeding time period.
$converted_i$	Area (ha) of habitat i that converted to open water during the preceeding time period.
Soil carbon density	years of belowground soil carbon that has accumulated in the top 1 m of soil.
dT	Length of the preceeding time period in years

COASTAL LOUISIANA CALCULATIONS

Future landscape projections for the entire Louisiana coast were not available from the numerical model used for the sub basin and basin-scale analyses. Therefore, the sensitivity analysis at the coastal Louisiana scale used physical input data from the numerical model used for the Louisiana Coastal Master Plan. The primary modeled land and habitat area for years 2020 through 2050 for all of coastal Louisiana were from the Integrated Compartment Model (ICM; Brown et al., 2017; Meselhe et al., 2013, 2017, 2021; White et al., 2017) results for the future without action (FWOA) scenario of the 2017 Louisiana Coastal Master Plan (CPRA, 2012, 2017, 2023). Using this coastwide model output, results presented in Figure 9 and Figure 10 calculated both net carbon flux and relative sensitivity as described above.

Previous studies have calculated net carbon flux across the Louisiana coast. To enable a comparison of these methodologies, we recalculated the flux using three different approaches (our current research; Baustian et al., 2023; Baustian et al., 2024) but used the updated habitat flux values detailed in Table 1. The equations used to calculate net carbon flux coastwide in Baustian et al. (2023) track all landscape changes between periods of model output (2020, 2025, 2030, 2050) and then subtract the accumulated carbon emissions due to these changes at a single point in time. For example, if 5,000 ha of saline marsh converts to open water between 2030 and 2050, all the carbon emissions caused by this land loss are not incurred until 2050. In contrast, the approach used in this study and Baustian et al. (2024) annualized carbon emissions occurring after land loss due to AG biomass decay and BG soil carbon decay. Finally, this study uses an updated and more conservative calculation for estimating carbon emissions related to land loss (e.g., the conversion from vegetated habitats to saline open water) than previous calculations (Baustian et al., 2023; Baustian et al., 2024). Equations 5–7 consider the AG biomass and BG soil carbon that persists through land loss (100% - WVD% and 100% - SCD%, respectively) as previously sequestered carbon rather than newly (additional) sequestered carbon.

SENSITIVITY ANALYSIS

To calculate the net carbon flux for each grid cell (Eq. 3), several input parameters are required, some of which have high uncertainty due to lack of data (e.g., the percentage of soil organic carbon that is liberated and oxidized following marsh edge erosion) or known high levels of spatial and temporal variability (e.g., wetland CH_4 and N_2O flux). The current default values for these parameters and their rationales are detailed in **Table 3.** To assess the impact of varying these assumptions on the estimated net CO_2e flux across the study area, we performed eFAST analyses (Saltelli et al., 1999) using the GlobalSensitivity (v2.7.0) package (Dixit & Rackauckas, 2022). eFAST is a variance-based sensitivity analysis that uses Fourier decomposition (Cukier et al., 1977) to test thousands of different input parameter combinations and quantify how changes in each input parameter—both individually and through interactions with other parameters—would contribute to variability or uncertainty in net carbon flux estimates (Eq. 3). This approach allows a distribution of all possible values to be considered for each parameter, rather than a single estimated or average value, and provides a comprehensive evaluation of how sensitive the net carbon flux calculations are to uncertainties in each of the input parameters.

For the analysis, eFAST was configured with a search curve that sampled the input parameter space 15,000 (n) times for each parameter (p), ensuring broad coverage of possible input combinations (Ryan et al., 2018). To reduce the large computational expense of conducting eFAST with 120,000 model iterations ($n \times p$), the net carbon flux calculation module was coded in Julia (Bezanson et al., 2012) and refactored to leverage GPU-acceleration through the CUDA (v5.5.2) package (Besard et al., 2019), decreasing eFAST simulation times from ~45 days to 1.9 hours when executed on an NVIDIA RTX 2070 Super GPU. The search curves were set to sample from uniform distributions for parameters 1 through 5, allowing each parameter to take any value between 0% and 100% (**Figure 2**). Search curves for parameters 6 through 8 were instead set to sample from normal distributions specific to each habitat (**Figure 2**). These normal distributions were defined using the mean and standard deviations from published values as shown in Table 1, allowing the carbon flux calculation module to sample the full variability of each habitat's ANPP, SCA, or GHG rates.

First Order (S_1) sensitivity indices were calculated for each input parameter for each model period to quantify the individual direct effect of each parameter uncertainties on net carbon flux uncertainty over time. Total Order (S_T) sensitivity indices—which captures the total contribution of an input parameter, including both its direct effects and all interactions with other input parameters—were also calculated but are not shown as S_T indices were similar to S_1 in all cases. Some parameter uncertainties result in skewed or heavy-tailed net carbon flux distributions, therefore net carbon flux uncertainty attributable to parameter uncertainty was summarized using interquartile ranges (IQR: 75th percentile minus 25th percentile) instead of the full range of data (maximum minus minimum), providing more stable estimates that are robust to outliers and distributional assumptions.

Table 3. *Assumed input parameters surrounding the consequences of various habitat conversion and coastal land loss scenarios on net carbon flux calculations. Bold, underlined values denote current default values for these calculations.*

#	Parameter	Assumptions	References
1	herbaceous wetland SCD%	When herbaceous wetland habitats convert to open water, the **top ~1 m of soil** is assumed to erode. A portion of the stored carbon in this eroded soil horizon is decomposed to CO_2 by aerobic microorganisms. Grass, rush, and sedge-derived soil organic matter is relatively labile, and thus microbial decomposition is rapid: <u>**75%**</u> of the carbon stored in the eroded soil is assumed to decay to atmospheric CO_2 before it can be reburied into anoxic sediment horizons whereupon aerobic decomposition then halts.	(EPA, 2024; McTigue et al., 2021; Pendleton et al., 2012; Sapkota & White, 2019)

2	woody habitat SCD%	When woody habitats (e.g. mangrove forests) convert to open water, the **top ~1 m of soil** is assumed to erode. Soil organic matter derived from woody wetland vegetation is typically lignin-rich, and thus microbial decomposition is slower than for soil organic matter derived from herbaceous vegetation: **50%** of the eroded soil's carbon stock is assumed to decay to atmospheric CO_2 before it is reburied into anoxic sediment horizons whereupon aerobic decomposition halts.	(EPA, 2024; Kristensen et al., 2008)
3	Soil carbon density	The amount of stored soil carbon that becomes vulnerable to microbial decomposition after a habitat converts to open water depends on how many years of accumulated carbon were stored in the eroded soil horizon. Based on vertical accretion rate data (0.53 cm yr^{-1}) collected in Barataria Bay, the top 1 m of soil is assumed to store **189 years** of accumulated soil carbon.	(Baustian et al., 2021)
4	HVD%	When marsh habitats convert to open water, all aboveground vegetation is assumed to die. **100%** of this biomass is assumed to decay to atmospheric CO_2.	(EPA, 2024)
5	WVD%	When woody habitats (e.g. mangrove forests) convert to herbaceous wetland or open water, 50% of the aboveground biomass is assumed to remain sequestered in ghost trees, while **50%** decays to atmospheric CO_2.	(Baustian et al., 2024; Krauss et al., 2018)
6	Open saline water soil carbon accumulation rate (tons CO_2e ha^{-1} yr^{-1})	Soils in saline open waters accumulate carbon from the deposition of terrestrial organic material, lateral flux of eroded marsh material, and/or sedimentation of marine primary production. This is assumed to occur at a rate of **-8.0 tons of CO_2e ha^{-1} yr^{-1}**.	(Hillmann et al., 2020; Smith et al., 1983)
7	CH_4 and N_2O flux	CH_4 and N_2O flux estimates for each habitat were assumed to be the annual mean values derived from a review of published flux measurements. These mean values are habitat specific and appear in Table 1.	(Al-Haj & Fulweiler, 2020; Baustian et al., 2024)
8	ANPP	ANPP estimates for each habitat were assumed to be the annual mean values derived from a review of published ANPP measurements. These mean values are habitat specific and appear in Table 1.	(Baustian et al., 2023; Ewe et al., 2006)

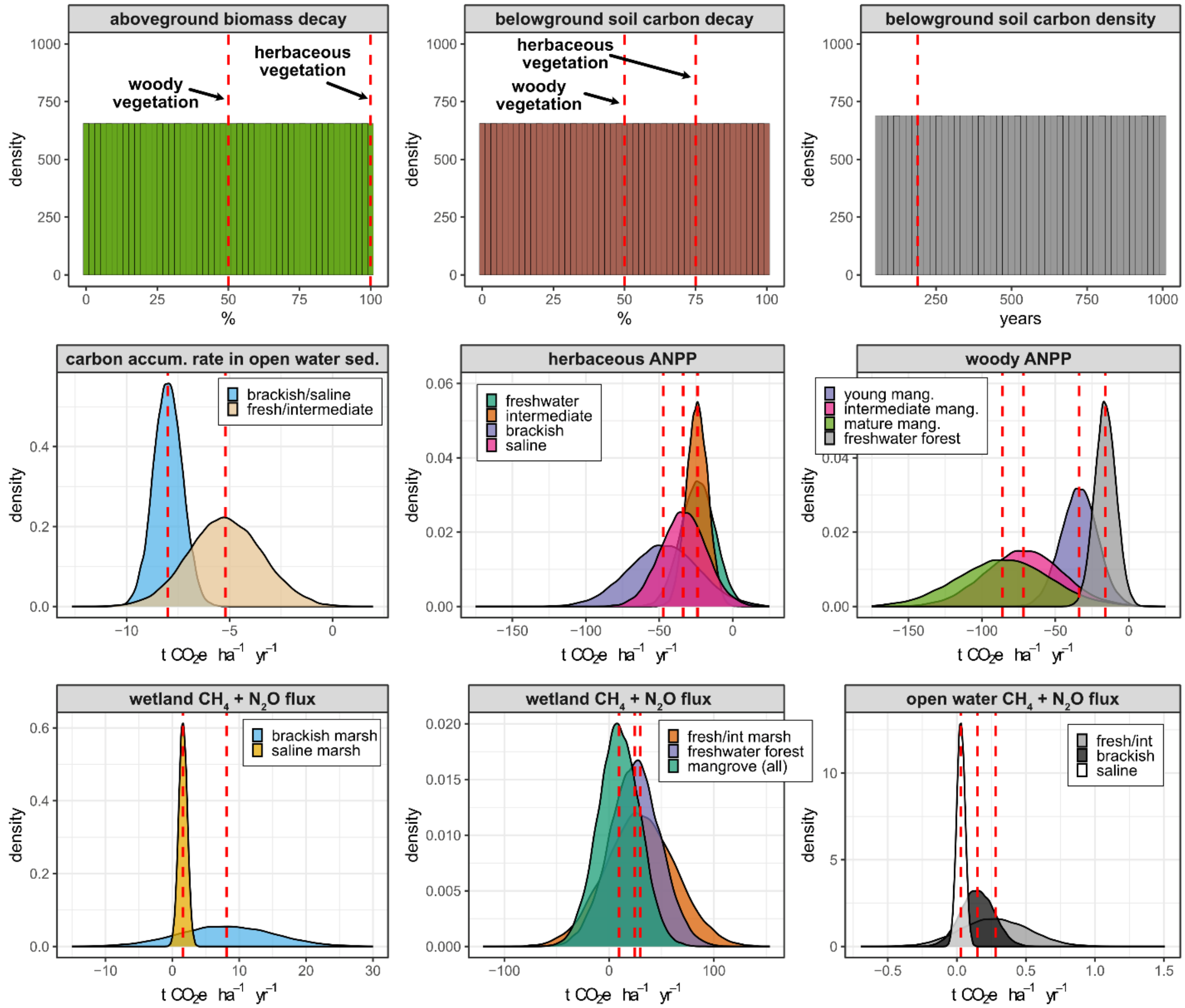

Figure 2. *Visualization of the known or estimated variation for each input parameter within the net carbon flux calculations. Dashed red lines denote the current default value for each input parameter for net carbon flux calculations described in this study. Colored histograms and density plots represent the total input space tested in the eFAST simulations (distributions are uniform or represent the normal distribution based on the mean ± 1 sd from literature values).*

RESULTS

SUB BASIN SCALE

Changes in the landscape and habitats surrounding Port Fourchon were modeled with Delft3D-FM over a 30-year period (**Figure 3**), revealing significant shifts driven by salinity changes, loss of vegetation, wetland erosion, and open water expansion during that time period. Modeled losses of saline marsh habitats were concentrated to the east and northeast of Port Fourchon. In total, saline marshes declined in areal coverage by 52% within the study area by 2050, shrinking from 10,685 ha to 5,591 ha. Most of this saline marsh loss was replaced with open water habitat, which expanded from 46,092 ha in 2020 to 51,791 ha by 2050 (**Table 4**). Brackish marshes located in the northern limit of the study area decreased from 356 ha to 66 ha, with most eroding into open water or converting to saline marsh as salinity increased (an increase of 1–3 psu in 2050 compared to 2020). In the south, young, intermediate, and mature mangrove forests initially occupied 234 ha, 223 ha, and 711 ha, respectively, and gradually transitioned into saline herbaceous marsh by 2030. However, by 2050, this new saline herbaceous marsh also transitions to open water. Overall, the combined areal coverage of mangrove forests decreased by 31% to 853 ha.

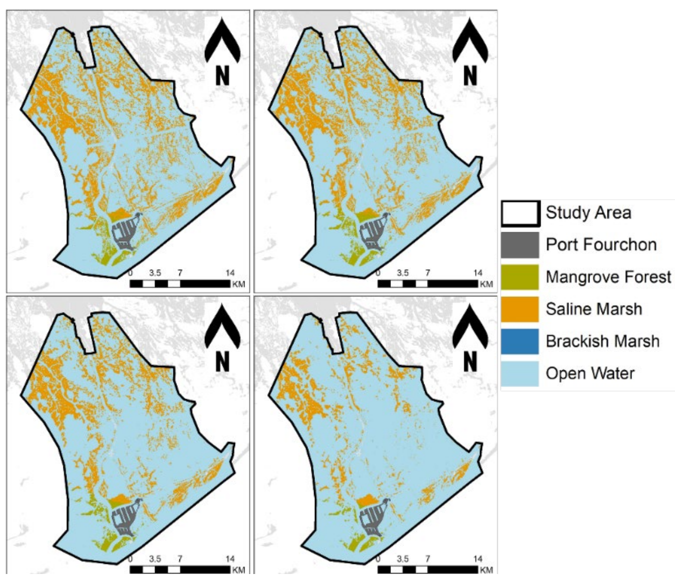

Figure 3. *Modeled emergent land and open water habitat changes surrounding Port Fourchon for 2020, 2025, 2030, and 2050. Landscape color denotes the dominant habitat type with the highest percent cover within each grid cell. The black border denotes the boundary of the study area.*

__Table 4.__ Changes in habitat areas within the Port Fourchon case study area (black border in Figure 3).

Habitat	Area (ha)			
	2020	2025	2030	2050
brackish marsh	356	203	123	66
saline marsh	10,685	10,044	8,724	5,591
young mangrove forest	234	247	231	171
intermediate mangrove forest	223	234	247	231
mature mangrove forest	711	756	678	451
open water (saline)	46,092	46,817	48,298	51,791
Total	58,301	58,301	58,301	58,301

The land water and habitat classifications in the first year of the model simulation ('2020') was based on a 2014 land use land cover map (Couvillion, 2017) and was used as the boundary condition or baseline from which land losses in subsequent years were dynamically modeled. As such, net carbon flux estimates for the Port Fourchon area in 2020 did not model any land loss effects and were thus insensitive to land loss related parameters. Net carbon flux uncertainty in 2020 was thus driven only by uncertainties in ANPP (S_1 = 79.0%) and CH_4 and N_2O fluxes (S_1 = 15.8%; **Figure 4**). Considering these uncertainties in terms of the potential impact upon net carbon flux, this represents an IQR of 0.38 MMT CO_2e per year in net carbon flux estimates due to current ANPP uncertainties and an IQR of 0.17 MMT CO_2e per year in net carbon flux estimates due to CH_4 and N_2O flux uncertainties (**Figure 5**). However, with the inclusion of land loss and associated carbon flux to the atmosphere, the relative importance of ANPP, CH_4, and N_2O flux uncertainties decline over time. By 2050, nearly half of the existing herbaceous wetland habitat in the Port Fourchon area is projected to have converted to open water, and consequently, uncertainty in net carbon flux estimates for 2030 and 2050 were driven almost entirely by: (1) *soil carbon density*, which estimates the total amount of belowground soil carbon stored in the top ~1 meter of soil (S_I = 39.2%), and (2) *% soil carbon loss (herbaceous)*, the percentage of this belowground soil carbon that decays to atmospheric CO_2 when this top ~1 meter of soil is eroded during wetland degradation and conversion (S_I = 42.5%). On the carbon flux scale, net carbon flux variability due to uncertainties surrounding the extent and fate of eroded soil carbon becomes increasingly large as land loss accumulates, peaking at an IQR of 1.71 MMT CO_2e per year in 2030 (Figure 5, middle).

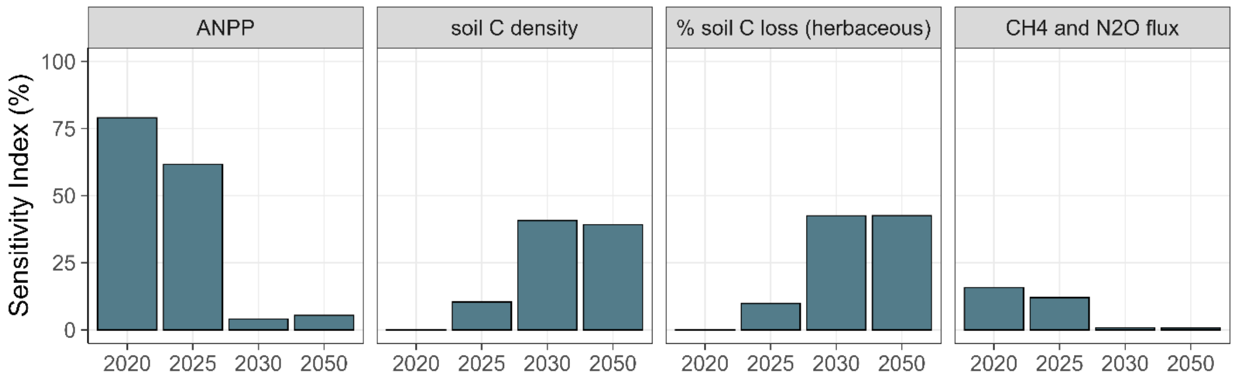

Figure 4. *Net carbon flux estimates across the Port Fourchon area were most sensitive to ANPP uncertainty over short times scales, but were eventually dominated by uncertainties surrounding the magnitude and ultimate fate of soil carbon stores that erode during coastal land loss processes. Navy bars: first-order (S_1) sensitivity indices. For brevity, parameters with sensitivites indices <5% for every modeled year are not shown.*

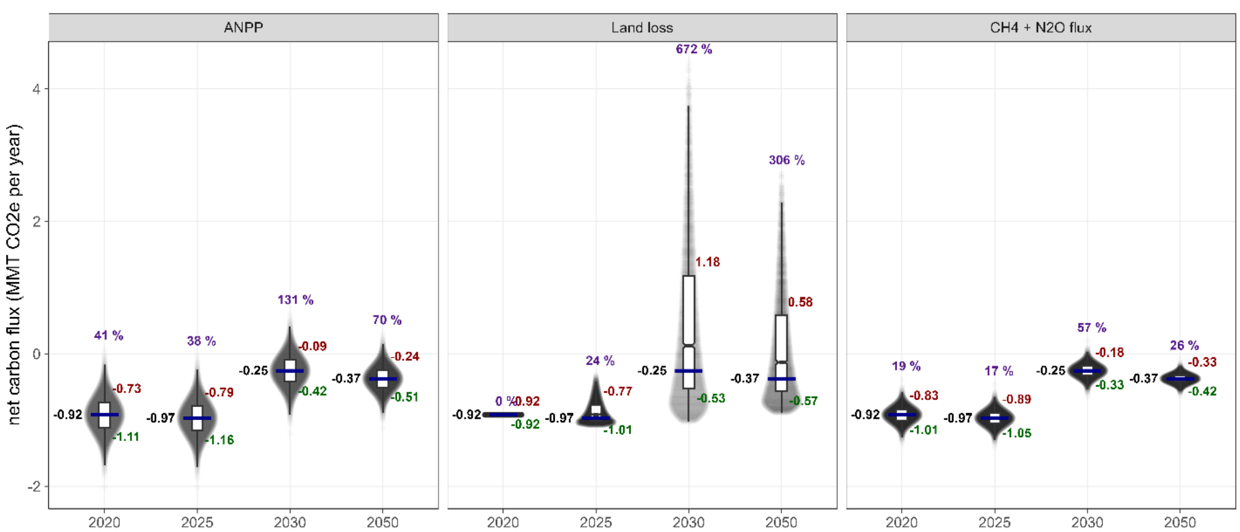

Figure 5. *Each panel displays the probability density of possible net carbon flux estimates due to the uncertainty in an input parameter using 2^{12} quasi-random samples. Red and green numbers indicate the 75^{th} and 25^{th} net carbon flux quartiles for each simulation. Horizontal blue lines with black numbers are references that denote the calculated net carbon flux across Port Fourchon if using the current default value for all input parameters. Purple numbers denote the relative (%) uncertainty, calculated as the interquartile range divided by the calculated flux using default values (black number).*

BASIN SCALE

For the basin scale analysis, changes in the landscape and habitats within Barataria Basin were projected over a 30-year period (**Figure 6**). In these Delft3D-FM model runs, habitat shifts are concentrated predominantly in the southern half of the basin, largely due to high rates of land loss. Saline marshes reduce in areal coverage by 43% within Barataria Basin by 2050, a loss of 11,699 ha. Most of this loss is due to transition of emergent saline marsh to brackish or saline open water, which expands in area by 40.7% and 7.1% (**Table 5**). Brackish marshes located in the middle of Barataria Basin expand slightly from 18,499 ha to 20,098 ha, mostly due to marsh submergence resulting from relative sea level rise. Mangrove forests are relatively rare within Barataria Basin, occupying a mean of 294 ha across all age groups in the south of the study area, they reduce by ~54% to only 136 ha by 2050.

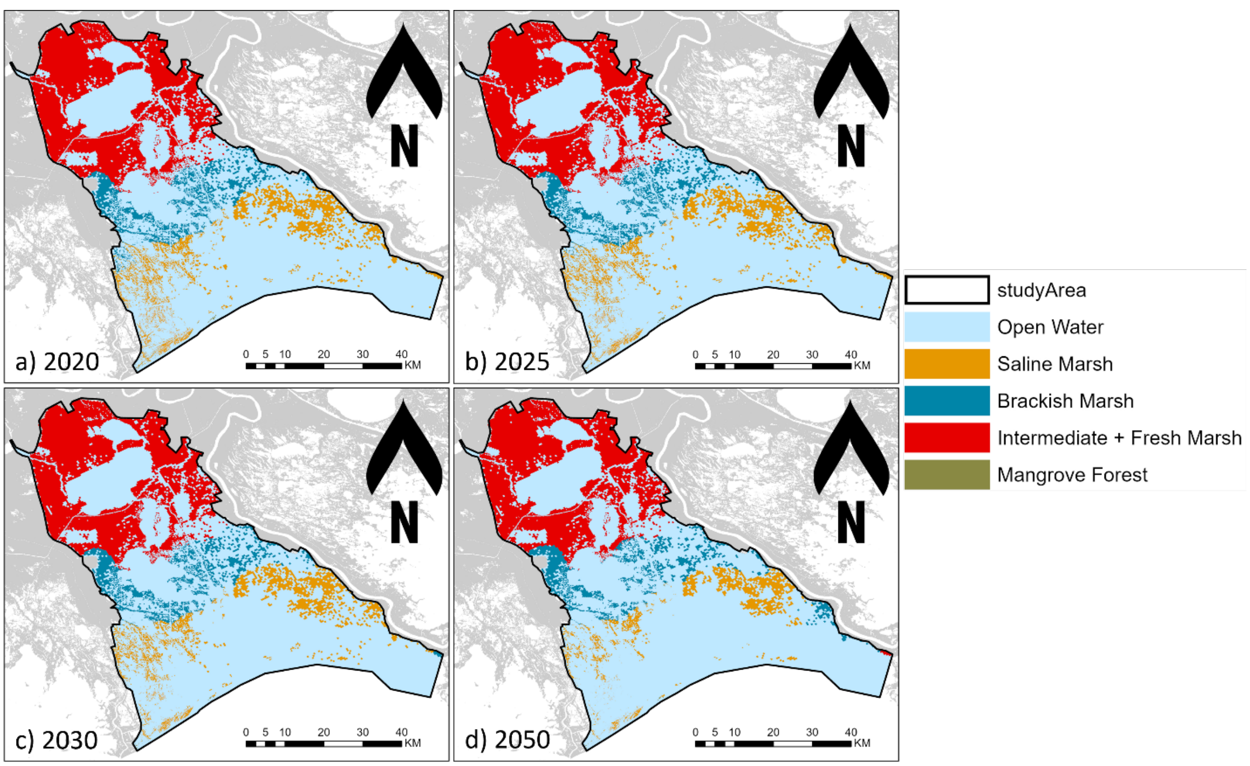

Figure 6. *Predicted landscape and habitat changes in Barataria Basin for 2020, 2025, 2030, and 2050. Landscape color denotes the habitat type with the highest % cover of each grid cell. The black line denotes the boundary of the study area.*

Table 5. *Changes in habitat areas within the Barataria Basin study area (Figure 6)*

Habitat	Area (ha)			
	2020	2025	2030	2050
freshwater marsh	5 244	4 356	3 855	3 440
intermediate marsh	69 454	70 723	70 602	67 910
brackish marsh	18 499	18 852	18 920	20 098
saline marsh	27 100	25 664	23 935	15 401
young mangrove forest	184	41	37	27
intermediate mangrove forest	22	164	41	37
mature mangrove forest	88	0	106	72
bare ground	308	1202	1202	1202
open water (fresh)	48 738	46 589	45 156	41 103
open water (intermediate)	6 871	7 705	7 707	4 723
open water (brackish)	28 657	29 407	29 358	40 308
open water (saline)	151 660	152 121	155 907	162 503
Total	356 825	356 825	356 825	356 825

Separate eFAST analyses for Barataria Basin net carbon flux estimates were performed for each salinity regime. In freshwater areas (both marsh and open water), net carbon flux uncertainty did not shift significantly over time and was driven primarily by CH_4 and N_2O flux uncertainty (S_1 = 49.0% ± 3.5%; mean ± sd) followed by the uncertainty in ANPP (S_1 = 32.5% ± 1.6%) and carbon accumulation rate in open water sediments (S_1 = 14.3% ± 1.9%). In terms of the potential impact upon net carbon flux, the magnitude of net carbon flux uncertainty due to these parameters was small with an average IQR across all parameters of only ~0.08 MMT CO_2e per year, reflecting the relatively small areal extent (~4,200 ha) of freshwater marsh habitats in Barataria Basin.

In intermediate marsh habitats—which is the most extensive vegetated habitat type by area within Barataria Basin (Table 5)—the importance of ANPP uncertainty is low (S_1 = 4.5% ± 0.03%) compared to other salinity regimes (Figure 7). In these areas of Barataria Basin, CH_4 and N_2O flux is the dominant driver of net carbon flux uncertainty (S_T ≈ 91.2% ± 0.02%). In terms of net carbon flux, uncertainty in net carbon flux attributable to CH_4 and N_2O flux uncertainties has an IQR ≈ 3.16 MMT CO_2e per year, representing 521% of the median net carbon flux estimate.

In brackish and saline marsh habitats, ANPP uncertainty is the primary source of net carbon flux uncertainty over short-time scales or in scenarios where land loss is limited (S_1 > 82%, average IQR ≈ 0.79 MMT CO_2e per year). However, as coastal land loss accumulates in Barataria Basin, net carbon flux sensitivity to ANPP uncertainties decreases to 56% (brackish) and 21% (saline) as the importance of soil carbon density and % soil carbon loss parameters uncertainties increase. In terms of net carbon flux, uncertainty attributable to land loss has an IQR of 0.57 MMT CO_2e per year in brackish habitats and 1.57 MMT CO_2e per year in saline habitats.

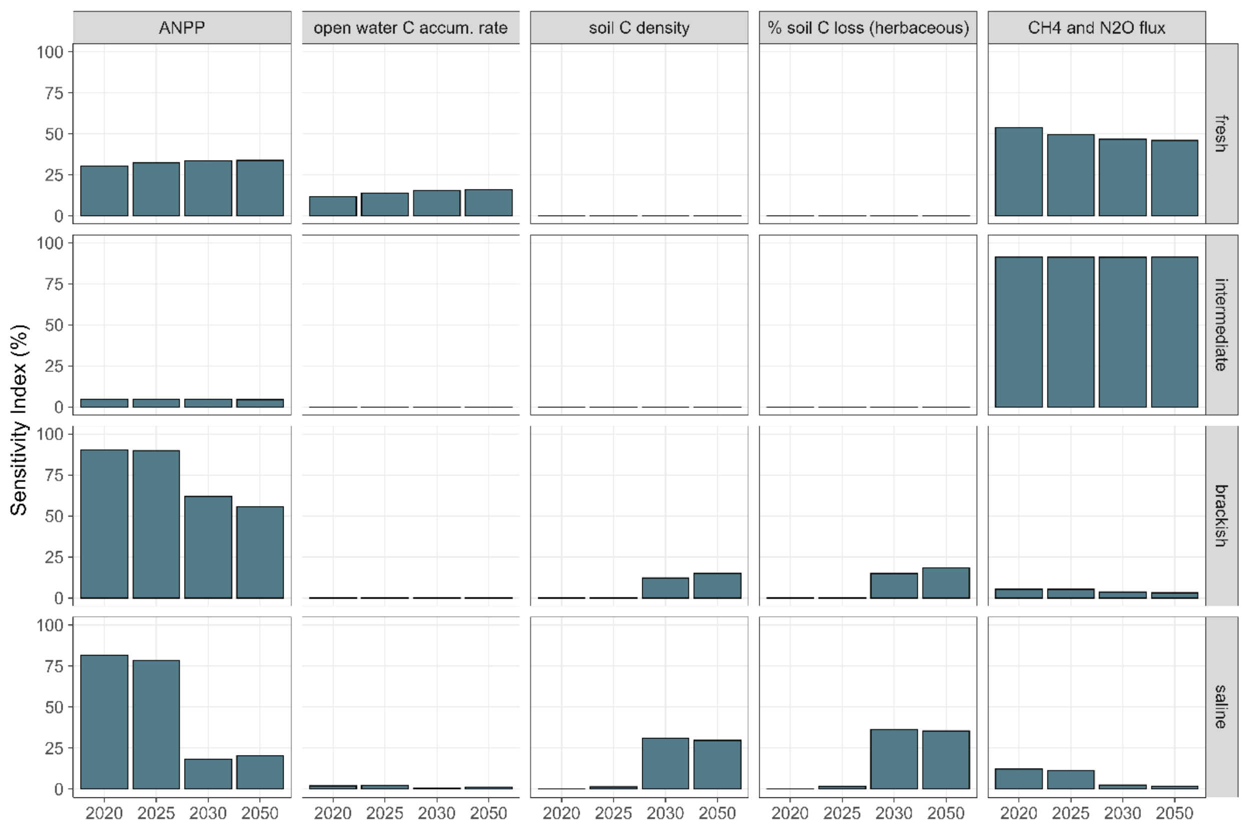

Figure 7. *First-order sensitivity indices for the input parameters used to estimate net carbon flux across Barataria Basin. For brevity, parameters with sensitivities indices <5% for every modeled year are not shown. Total areas for each salinity regime (emergent wetland + open water) are shown in Table 5.*

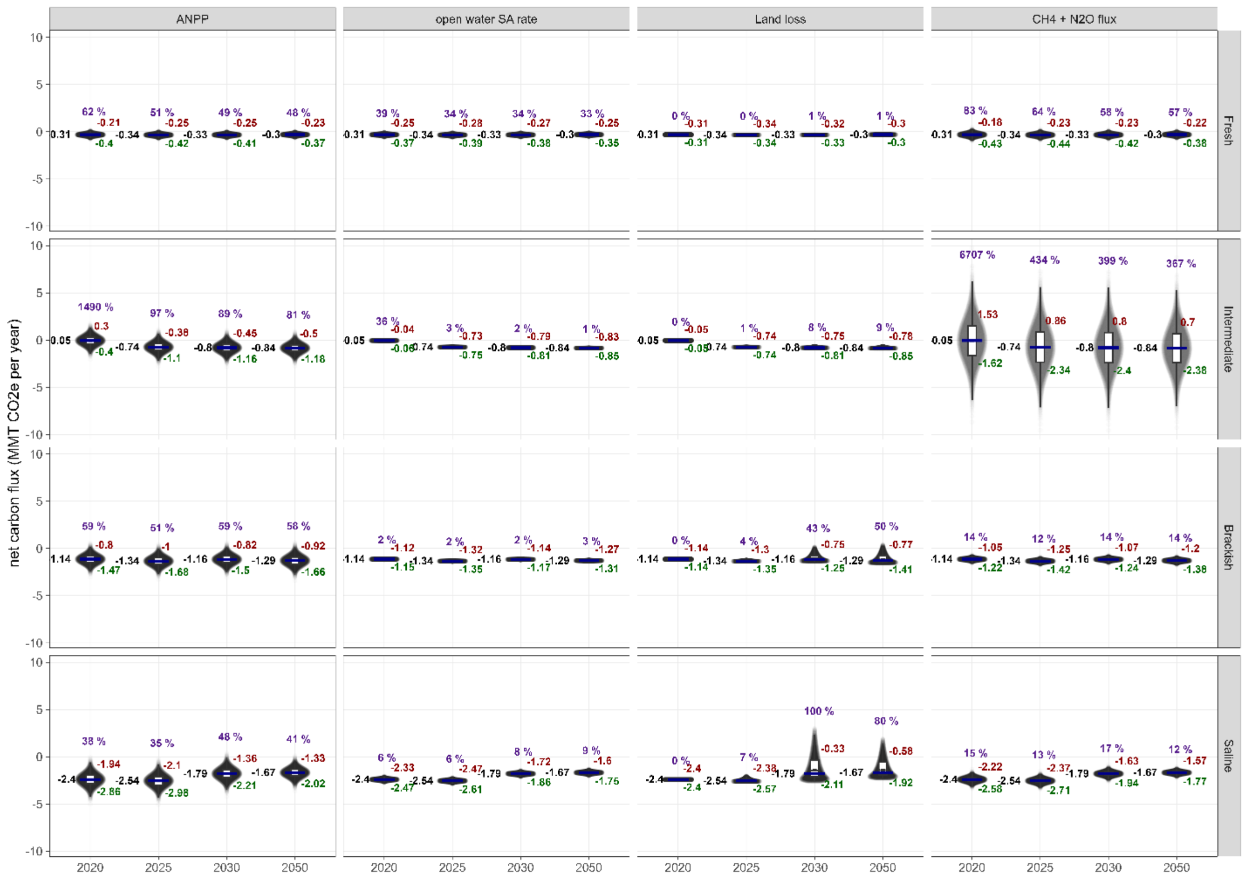

Figure 8. *Each panel displays the range net carbon flux estimates across Barataria Basin. Each plot was calculated using 2^{12} quasi-random samples from that panel's input parameter's input space. Red and green numbers indicate the 75th and 25th net carbon flux quartiles for each simulation. Horizontal blue lines with black numbers are references that denote the calculated net carbon flux for each salinity regime within Barataria Basin if using the current default value for all input parameters. Purple numbers denote the relative (%) uncertainty, calculated as the interquartile range divided by the calculated flux using default values (black number).*

COASTAL ECOSYSTEM SCALE

For the coastal ecosystem scale analysis, changes in the landscape and habitats within coastal Louisiana over a 30-year period from the ICM model outputs from the 2017 Louisiana Coastal Master Plan were used (CPRA, 2017; White et al., 2017). At all times analyzed over the 30-year period, uncertainty in net carbon flux estimates was approximately 64% due to uncertainty in CH_4 and N_2O flux, and 28% due to uncertainty in ANPP (Figure 9). Uncertainty around quantifying carbon loss with transition of emergent marsh to open water was a minor contribution to overall uncertainty in estimating net carbon flux, except 30 years in the future (2050) when land loss is projected to accelerate due to sea level rise (Figure 9; CPRA, 2017).

Considering these uncertainties in terms of the potential impact upon net carbon flux estimates at a coastwide scale, $CH_4 + N_2O$ flux represents a mean uncertainty (IQR) of 118% and ANPP represents a mean uncertainty (IQR) of 81% (**Figure 10**). Quantifying that as metric tons of carbon, the mean net storage of 43 MMT CO_2e per year could conservatively (75th and 25th percentile) be as little as a net storage of 18 MMT CO_2e per year or as high as 68 MMT CO_2e per year, solely based on the uncertainty in CH_4 and N_2O flux (Figure 10). Similarly, uncertainty in ANPP alone could mean that the estimated 43 MMT CO_2e per year could conservatively (75th and 25th percentile) be as little as a net storage of 25 MMT CO_2e per year or as high as a storage of 60 MMT CO_2e per year (Figure 10).

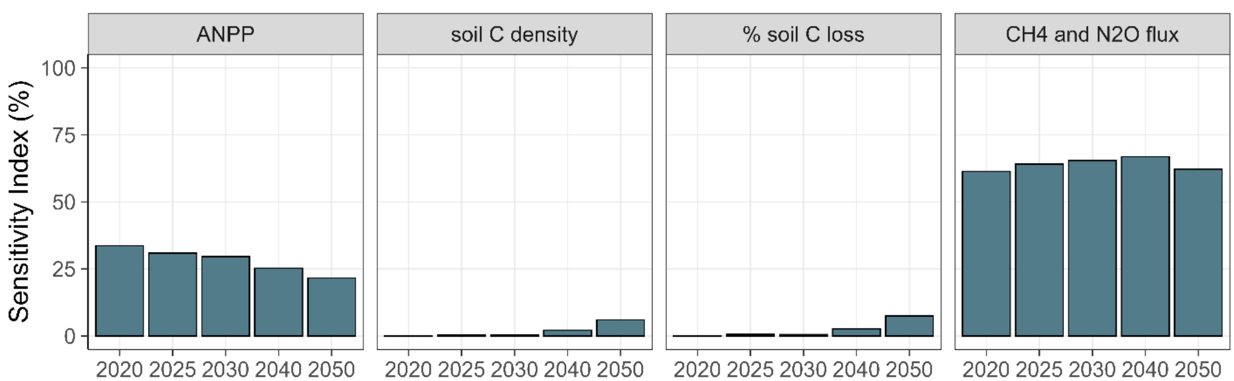

***Figure 9**. First-order sensitivity indices for the input parameters used to estimate net carbon flux across coastal Louisiana. For brevity, parameters with sensitivities indices <5% for every modeled year are not shown.*

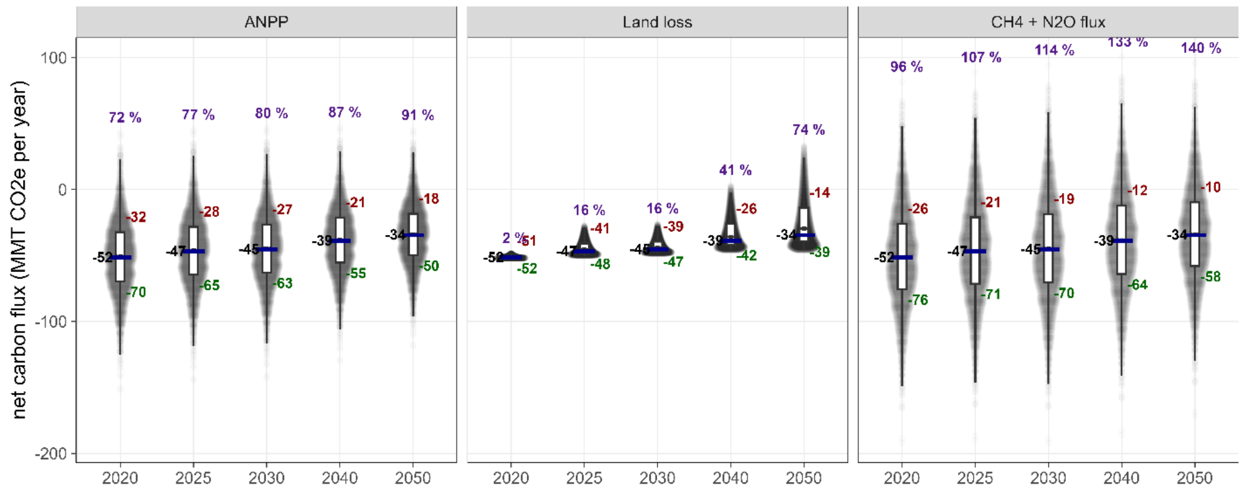

Figure 10. *Each panel displays the probability density of possible net carbon flux estimates due to the uncertainty in an input parameter using 2^{12} quasi-random samples. Red and green numbers indicate the 75th and 25th net carbon flux quartiles for each simulation. Horizontal blue lines with black numbers are references that denote the calculated net carbon flux across coastal Louisiana if using the current default value for all input parameters. Purple numbers denote the relative (%) uncertainty, calculated as the interquartile range divided by the calculated flux using default values (black number).*

The estimation of net carbon flux from coastal Louisiana is strongly influenced by nuances in the calculation approach. When land loss was accumulated over the variable model output periods, the results indicate that coastal Louisiana could become a net source of carbon by 2050 (Baustian et al., 2023), which is not the case in the updated calculations where land loss was calculated to an annual uniform rate (Baustian et al., 2024). Similarly, the current study confirms that coastal Louisiana will remain a net sink of carbon through 2050. The update in the current study over Baustian et al., 2024 resulted in a ~10% reduction in estimate of net carbon flux from coastal Louisiana in 2050 (Table 6).

Table 6. *Estimates of net carbon flux for coastal Louisiana based on outputs of future land area and habitat from the 2017 Louisiana Coastal Master Plan, comparing quantification approaches for estimating land loss emissions from this study with Baustian et al., 2023 and Baustian et al., 2024.*

Arithmetic approach	**Method**	**Louisiana Coastwide Carbon Flux (MMT CO_2e yr^{-1})**				
		2020	**2025**	**2030**	**2040**	**2050**
current study	Land loss emissions annualized, updated and more conservative land loss carbon flux calculation (equations 5-7)	-51.51	-46.90	-45.33	-38.87	-34.49
Baustian et al. 2024	Land loss emissions annualized	-51.71	-48.10	-46.58	-41.29	-38.37
Baustian et al. 2023	Land loss emissions accumulated since the previous model year	-46.39	-38.63	-37.30	+3.92	+35.04

DISCUSSION

The accurate quantification of net carbon flux across landscapes represents a fundamental challenge for blue carbon project developers and carbon resource managers. Although coastal ecosystems have exceptional potential to remove and sequester carbon from the atmosphere, accurate and verifiable quantification of this capacity is still lacking compared to green carbon ecosystems due to uncertainties surrounding the dynamic processes and land-water interactions that are inherent to coastal ecosystems. This is particularly true for herbaceous wetlands in eroding coastlines with highly variable salinity. These uncertainties, among others, include errors and biases in measuring annual vegetation productivity at landscape scale across different plant community types, high variability in methane and nitrous oxide fluxes, and high uncertainty in the magnitude of carbon emissions produced during coastal land loss (Pendleton et al., 2012; Rosentreter et al., 2018, 2021; Roth et al., 2022). Systematically identifying which of these uncertainties most significantly impact net carbon flux estimates across multiple spatial and temporal scales—from localized regions to entire coastal basins—has remained a challenge.

This study reveals how the relative importance of blue carbon flux uncertainty varies depending on wetland type, salinity regime, and both the spatial and temporal scale of quantification. Potential emissions from eroded soil carbon due to land loss can be an enormous source of net carbon flux uncertainty, but may take decades to manifest, whereas high variability in ANPP or methane (CH_4) and nitrous oxide (N_2O) fluxes can have more immediate effects. Moreover, the significance of these uncertainties is not uniform across all scenarios. While net carbon flux may be highly sensitive to variances in CH_4 and N_2O fluxes, the relative importance of addressing these uncertainties may be low if habitats with highly variable CH_4 and N_2O fluxes (e.g. freshwater marshes) represent a relatively small percentage of the project footprint or are overshadowed by other uncertainties. By quantifying the contribution of uncertainty in individual parameters to overall uncertainty in net carbon flux estimates, this study offers a strategic roadmap of when and where targeted research and/or monitoring efforts will be most impactful.

ANPP

Aboveground net primary productivity (ANPP) was indicated as a large source of uncertainty across multiple spatial and temporal scenarios, especially over shorter time frames or in regions with slower coastal land loss rates. Much of this uncertainty arises from inherent errors and biases that arise when estimating ANPP at the landscape scale across diverse habitat types, all of which can be differentially impacted by storm events and seasonal variations in temperature and precipitation. Developing accurate, high-resolution mapping and validated predictions of existing vegetation types and their spatiotemporal variations will help reduce this uncertainty. Leveraging multi- and hyper-spectral imaging, LiDAR, and/or other remote sensing technologies may represent a pathway for project developers to enhance measurement accuracy and potentially increase the yield of certified carbon credits produced by a project (Carruthers et al., 2024; Macreadie et al., 2022). Such an approach is likely to offer the best benefit-cost ratio for smaller-scale blue carbon projects where detailed mapping of plant species across the whole project area is more achievable. Drone-based surveys enable small-scale project developers to more precisely estimate annual aboveground biomass within specific project areas (Almeida et al., 2019; Cunliffe et al., 2020; de Castro et al., 2021; Harris et al., 2024; Robinson et al., 2022), reducing net carbon flux uncertainties. For developers managing larger, geographically distributed blue carbon portfolios, satellite-based remote sensing provides lower resolution but scalable alternative to drone-based surveys (LaRocque et al., 2020; Zhang et al., 2022).

CARBON EMISSIONS FROM COASTAL WETLAND LAND LOSS

Given the substantial amount of coastal land loss projected through 2050, the potential emission of centuries to millennia of stored carbon could be a significant contributor to net carbon emissions over the lifespan of a blue carbon project in Louisiana (Mitra et al., 2005; Warnell et al., 2022). Soil data from the Louisiana Coastal Reference Monitoring System (CRMS) indicate belowground soil carbon stocks of Louisiana's coastal wetlands are highly spatially variable: Organic matter content in the top 24 cm alone ranges from as low as 3.7% to as high as 81.7% (Wang et al., 2017). This variability is mirrored in a recent projection of wetland soil organic carbon (SOC) stocks that predicts the top 1m of tidal marsh soils contain on average 985 ± 421 tonnes of CO_2e per hectare globally (Maxwell et al., 2024), a coefficient of variation of ~43%. Converting this value to an annual rate using the average SCA across coastal Louisiana, there are 131 ± 56 years of accumulated carbon in the top 1 m of soil, ignoring compaction, comparable to the 189 years estimated by (Baustian et al., 2023).

The extent to which eroded soil carbon is oxidized by microorganisms following wetland loss is highly uncertain, even more than the uncertainty of soil carbon stocks themselves. In this study, the default assumption was that 75% of herbaceous marsh and 50% of mangrove forest soil carbon stocks are lost to the atmosphere upon conversion to open water (Baustian et al., 2023; Sapkota & White, 2019). However, this rate of oxidation is highly uncertain, likely highly spatially and temporally variable, and potentially influenced by a range of factors such as vegetation community type, microbial community composition, temperature, salinity, and dissolved oxygen concentrations. Moreover, the classic decay model of soil carbon degradation—where rates initially rise and then slow down as labile substrates are depleted (Melillo et al., 1989)—has been challenged by evidence of rapid degradation of even recalcitrant organic matter following marsh edge erosion (Steinmuller et al., 2019). Furthermore, the physical movement and transport of eroded material play a crucial role, as there are plausible scenarios where eroded soil is rapidly reburied on the marsh platform before significant microbial decomposition can occur (Hopkinson et al., 2018). This potential for reburial introduces a finite time window during which eroded belowground soil carbon can decay (McTigue et al., 2021). Given these interacting uncertainties, this study made no specific assumption about the extent of decay and instead tested the full range from 0% to 100%. Previous, slightly more conservative, estimates from Monte Carlo simulations of global seagrass, tidal marsh, and mangrove losses have tested decay rates of between 25% and 100% soil carbon loss during habitat conversion (Pendleton et al. 2012).

There is a critical need to empirically assess soil carbon loss rates in the field across salinity gradients in Louisiana. Current standards for certifying carbon offset projects often compound these challenges by requiring developers to assume carbon fluxes that may underestimate net greenhouse gas project benefits. For example, the VM0033 standard dictates that a developer must conservatively assume that any coastal land loss results in 0% soil carbon loss under baseline scenarios, but 100% soil carbon loss within their project area (Emmer et al., 2015). Alternatively, direct monitoring of carbon emissions over the project's life is demanded. These mandatory assumptions or monitoring requirements are likely to make most blue carbon accreditation efforts in herbaceous tidal wetlands of dynamic coastal systems financially non-viable by increasing a developer’s monitoring costs beyond the total revenue generated by the project.

CH_4 AND N_2O FLUX

The flux of methane (CH_4) and nitrous oxide (N_2O) was the greatest source of uncertainty in net carbon flux estimates with CH_4 generally making up between 64% and 99% of this combined flux. The anoxic soil conditions that enhance the ability of blue carbon ecosystems to sequester and store carbon over long timeframes also favor the production of CH_4—especially in freshwater and oligohaline (i.e. salinity <5 ppt) environments (Al-Haj & Fulweiler, 2020; Poffenbarger et al., 2011). Given methane's high global warming potential—20 to 80 times that of CO_2 depending on the time horizon—even small emissions can shift a wetland from a net greenhouse gas sink to a source (Abernethy & Jackson, 2022; Balcombe et al., 2018; Dalmagro et al., 2019; Taillardat et al., 2020). This high variability is driven by a wide array of factors, including organic matter availability, plant productivity and community type, water saturation, temperature, and the presence of electron acceptors, leading to significant heterogeneity even between sites just tens of meters apart (Hanson & Hanson, 1996; Weston et al., 2014).

The immense spatial and temporal variability of methane flux makes it difficult to predict and poses a significant challenge for carbon accounting. Traditional process-based biogeochemical models developed for terrestrial or oceanic ecosystems are rarely useful in wetland ecosystems as methane flux from wetlands is difficult to predict based solely on environmental parameters. For decades, salinity has been used as a general predictor, with emissions expected to be low at salinities >20 ppt (Poffenbarger et al., 2011). However, its predictive power is weak; a recent meta-analysis found that salinity explained only 23% of methane flux variance in saltmarshes (Al-Haj & Fulweiler, 2020). This uncertainty is reflected in carbon offset methodologies like VM0033 (Emmer et al., 2015), which require project developers to either: (1) conduct intensive, costly field monitoring of methane emissions, (2) estimate them using a certified proxy or deterministic model that has been validated with direct methane measurements from a system with similar water table depth and dynamics, salinity, tidal hydrology, sediment supply and plant community, or (3) use highly conservative default values. These requirements are especially challenging for projects within the intermediate salinity regimes (0.5 – 18 PSU), where estimated emissions range over three orders of magnitude (0.003–5.39 T CH_4 ha^{-1} yr^{-1}), often rendering blue carbon projects in these areas economically non-viable.

A promising path to reducing this uncertainty may lie in moving beyond simple environmental parameters and incorporating microbial ecology. Methane production and consumption is the result of a complex metabolic network of interacting microorganisms, and many studies have shown that microbial community structure and activity can be as influential as soil chemistry in determining carbon dynamics (Allison, 2012; Allison et al., 2010; Blagodatsky & Richter, 1998; Fujita et al., 2014; Lawrence et al., 2009; Lehmann et al., 2020; McGuire & Treseder, 2010; Wieder, Allison, et al., 2015; Wieder et al., 2013; Wieder, Grandy, et al., 2015). Indeed, some of the microbial taxa with the greatest power to predict methane flux are not known to cycle methane directly (Meyer et al., 2020), reflecting the complex microbial pathways by which methane is produced and consumed. Since uncertainty in methane emissions is often a major source of uncertainty in net carbon flux estimates, incorporating analyses of the composition, community structure, and/or activity of microorganisms involved in the production and consumption of methane or its precursors may substantially improve efforts to model and project future methane emissions from Louisiana's wetlands (Carruthers et al., 2024).

CONCLUSION

Despite more than five decades of research on carbon cycling in coastal herbaceous wetlands, critical knowledge gaps continue to generate significant uncertainty in net carbon flux estimates for these dynamic systems. Our analyses demonstrate that when the quantified variability underlying commonly used default values is considered, net carbon flux estimates can vary by over 100%. This highlights a fundamental challenge with accounting methodologies that apply generalized assumptions across diverse spatial and temporal scales. The practical implications are substantial; even minor changes in assumptions can shift the estimated net carbon flux by millions of tonnes of CO_2 equivalent over a blue carbon project's lifespan. While this uncertainty is commonly managed with buffer pools, this approach can dramatically reduce the amount of accredited, saleable carbon—often to the point that many blue carbon projects are financially non-viable.

This analysis provides a strategic framework that researchers, carbon project developers, and resource managers can use to prioritize the research and monitoring efforts necessary to improve blue carbon quantification and maximize the climate mitigation potential of coastal restoration and protection efforts. Realizing the financial viability of carbon crediting in dynamic tidal wetlands will require new approaches that minimize monitoring costs while maximizing the precision of flux estimates. Key research areas to reduce uncertainty include developing more precise, high-resolution (tens of meters) measurement methodologies for diverse coastal habitats; improving the quantification of CH_4 and N_2O flux variability, for which modern microbial ecological techniques show high potential; and creating verifiable models of soil carbon dynamics both during and after coastal land transformations. Leveraging validated, large-scale morphological, hydrodynamic, and hydrological models will also be critical for targeting data gaps and maximizing creditable carbon from restoration projects.

Our findings show that parameters vary in their impact on net carbon flux uncertainty, and their relative importance can change over time. In the short term, uncertainties in ANPP and the fluxes of methane and nitrous oxide dominate. However, in areas where coastal land loss is expected to progress over the coming decades, uncertainties related to soil carbon density and the potential carbon losses associated with emergent wetland submersion and erosion become increasingly important. The benefit of reducing a specific parameter's uncertainty depends on each wetland ecosystem’s characteristics, the project's timescale, and the intended purpose of the calculation—for instance, national accounting versus project-level carbon accreditation. By strategically focusing on the most influential sources of uncertainty, research and monitoring efforts can more effectively reduce variance in carbon flux estimates. This targeted approach will enhance confidence in blue carbon accounting, thereby improving the viability of blue carbon accreditation as a potential mechanism for financing coastal wetland restoration and climate change mitigation efforts.

REFERENCES

Abernethy, S., & Jackson, R. B. (2022). Global temperature goals should determine the time horizons for greenhouse gas emission metrics. *Environmental Research Letters*, *17*(2), 024019. https://doi.org/10.1088/1748-9326/ac4940

Al-Haj, A. N., & Fulweiler, R. W. (2020). A Synthesis of Methane Emissions from Shallow Vegetated Coastal Ecosystems. *Global Change Biology*, *26*(5), 2988–3005. https://doi.org/10/ghsxth

Allison, S. D. (2012). A trait-based approach for modelling microbial litter decomposition. *Ecology Letters*, *15*(9), 1058–1070. https://doi.org/10/f34s84

Allison, S. D., Wallenstein, M. D., & Bradford, M. A. (2010). Soil-carbon response to warming dependent on microbial physiology. *Nature Geoscience*, *3*(5), Article 5. https://doi.org/10/ch747c

Almeida, D. R. A., Broadbent, E. N., Zambrano, A. M. A., Wilkinson, B. E., Ferreira, M. E., Chazdon, R., Meli, P., Gorgens, E. B., Silva, C. A., Stark, S. C., Valbuena, R., Papa, D. A., & Brancalion, P. H. S. (2019). Monitoring the structure of forest restoration plantations with a drone-lidar system. *International Journal of Applied Earth Observation and Geoinformation*, *79*, 192–198. https://doi.org/10/gm8bfz

Alongi, D. M. (2012). Carbon sequestration in mangrove forests. *Carbon Management*, *3*(3), 313–322. https://doi.org/10/ggj7hf

Alongi, D. M. (2020). Carbon balance in salt marsh and mangrove ecosystems: A global synthesis. *Journal of Marine Science and Engineering*, *8*(10), Article 10. https://doi.org/10/gngvh5

Balcombe, P., Speirs, J. F., Brandon, N. P., & Hawkes, A. D. (2018). Methane Emissions: Choosing the Right Climate Metric and Time Horizon. *Environmental Science: Processes & Impacts*, *20*(10), 1323–1339. https://doi.org/10.1039/C8EM00414E

Baustian, M. M., Jung, H., Liu, B., Moss, L. C., Foster-Martinez, M., Esposito, C. R., Georgiou, I. Y., Bregman, M. C., Di Leonardo, D. R., McMann, B., Hemmerling, S. A., & Miner, M. D. (2024). Current and future potential net greenhouse gas sinks of existing, converted, and restored marsh and mangrove forest habitats. *Restoration Ecology*, *32*(8), e14259. https://doi.org/10/g8trkp

Baustian, M. M., Liu, B., Moss, L. C., Dausman, A., & Pahl, J. W. (2023). Climate change mitigation potential of Louisiana's Coastal Area: Current estimates and future projections. *Ecological Application*.

Baustian, M. M., Stagg, C. L., Perry, C. L., Moss, L. C., & Carruthers, T. J. B. (2021). Long-term carbon sinks in marsh soils of coastal Louisiana are at risk to wetland loss. *Journal of Geophysical Research: Biogeosciences*, *126*(3), e2020JG005832. https://doi.org/10/grmtwt

Belshe, E. F., Sanjuan, J., Leiva-Dueñas, C., Piñeiro-Juncal, N., Serrano, O., Lavery, P., & Mateo, M. A. (2019). Modeling Organic Carbon Accumulation Rates and Residence Times in Coastal Vegetated Ecosystems. *Journal of Geophysical Research: Biogeosciences*, *124*(11), 3652–3671. https://doi.org/10/grnnkv

Besard, T., Foket, C., & De Sutter, B. (2019). Effective Extensible Programming: Unleashing Julia on GPUs. *IEEE Transactions on Parallel and Distributed Systems*, *30*(4), 827–841. IEEE Transactions on Parallel and Distributed Systems. https://doi.org/10/gf7rfk

Bezanson, J., Karpinski, S., Shah, V. B., & Edelman, A. (2012). Julia: A fast dynamic language for technical computing. *arXiv Preprint arXiv:1209.5145*.

Blagodatsky, S. A., & Richter, O. (1998). Microbial growth in soil and nitrogen turnover: A theoretical model considering the activity state of microorganisms. *Soil Biology and Biochemistry*, *30*(13), 1743–1755. https://doi.org/10/fdpmj7

Brown, S., Couvillion, B., Conzelmann, C., de Mutsert, K., Fischbach, J., Hunnicutt, C., McKelvy, M., Quibodeaux, P., Roberts, H., Rodigue, M., Schindler, J., Suir, K., Thomson, G., Visser, J., & White, E. (2017). *2017 Coastal Master Plan: Appendix C: Modeling Chapter 3—Modeling Components and Overview. Version Final* (p. 72). Coastal Protection and Restoration Authority. http://coastal.la.gov/wp-content/uploads/2017/04/Appendix-C_chapter3_FINAL_6.19.2017.pdf

Carruthers, T., Jones, B., Terrell, M., Scheibly, J., Player, B., Black, V., Ehrenwerth, J., Biber, P., Connolly, R., Crooks, S., Curole, J., Darnell, K., Dausman, A., DeJong, A., Doyle, S., Esposito, C., Friess, D., Fourqurean, J., Georgiou, I., … Waycott, M. (2024). Identifying and filling critical knowledge gaps can optimize financial viability of blue carbon projects in tidal wetlands. *Frontiers in Environmental Science*, *12*.

Couvillion, B. (2017). *2017 Coastal Master Plan Modeling: Attachment C3-27: Landscape Data. Version Final* (Nos. C3-27; p. 84). http://coastal.la.gov/wp-content/uploads/2017/04/Attachment-C3-27_FINAL_03.10.2017.pdf

CPRA. (2012). *Louisiana's Comprehensive Master Plan for a Sustainable Coast* (p. 192). Coastal Protection and Restoration Authority of Louisiana.

CPRA. (2017). *Louisiana's Comprehensive Master Plan for a Sustainable Coast* (p. 184). Coastal Protection and Restoration Authority of Louisiana. http://coastal.la.gov/wp-content/uploads/2017/04/2017-Coastal-Master-Plan_Web-Single-Page_CFinal-with-Effective-Date-06092017.pdf

CPRA. (2023). *Louisiana's Comprehensive Master Plan for a Sustainable Coast* (p. 100) [4th Edition, Draft Plan Release]. Louisiana Coastal Protection and Restoration Authority, the State of Louisiana.

Cukier, R. I., Levine, H. B., & Shuler, K. E. (1977). Nonlinear sensitivity analysis of multiparameter model systems. *The Journal of Physical Chemistry*, *81*(25), 2365–2366. https://doi.org/10/bjpmfw

Cunliffe, A. M., Assmann, J. J., Daskalova, G. N., Kerby, J. T., & Myers-Smith, I. H. (2020). Aboveground biomass corresponds strongly with drone-derived canopy height but weakly with greenness (NDVI) in a shrub tundra landscape. *Environmental Research Letters*, *15*(12), 125004. https://doi.org/10/gjk9nj

da Silva Copertino, M. (2011). Add coastal vegetation to the climate critical list. *Nature*, *473*(7347), Article 7347. https://doi.org/10/dctrjv

Dalmagro, H. J., Zanella de Arruda, P. H., Vourlitis, G. L., Lathuillière, M. J., de S. Nogueira, J., Couto, E. G., & Johnson, M. S. (2019). Radiative forcing of methane fluxes offsets net carbon dioxide uptake for a tropical flooded forest. *Global Change Biology*, *25*(6), 1967–1981. https://doi.org/10/c3nt

de Castro, A. I., Shi, Y., Maja, J. M., & Peña, J. M. (2021). UAVs for Vegetation Monitoring: Overview and Recent Scientific Contributions. *Remote Sensing*, *13*(11), Article 11. https://doi.org/10/gnj8gf

Deltares. (2019). *D-Flow Flexible Mesh Suite: User Manual* (p. 412) [Version 1.5.0]. Deltares.

Dietz, M. E., Liu, K., & Bianchette, T. A. (2018). Hurricanes as a major driver of coastal erosion in the Mississippi River Delta: A multi-decadal analysis of shoreline retreat rates at Bay Champagne, Louisiana (USA). *Water*, *10*(10), Article 10. https://doi.org/10/gp9wqt

Dixit, V. K., & Rackauckas, C. (2022). GlobalSensitivity. Jl: Performant and Parallel GlobalSensitivity Analysis with Julia. *Journal of Open Source Software*, *7*(76). https://doi.org/10/g8nrfz

Emmer, I., Needelman, B. A., Emmet-Mattox, S., Crooks, S., Megonigal, P. J., Myers, D., Oreska, M., McGlathery, K., & Shoch, D. (2015). *VM0033: Methodology for Tidal Wetland and Seagrass Restoration* (No. Sectoral Scope 14). Verified Carbon Standard. http://verra.org/wp-content/uploads/2018/03/VM0033-Tidal-Wetland-and-Seagrass-Restoration-v1.0.pdf

EPA. (2024). *Inventory of U.S. Greenhouse Gas Emissions and Sinks: 1990-2022* (No. EPA 430R-24004). https://www.epa.gov/ghgemissions/inventory-us-greenhouse-gas-emissions-and-sinks-1990-2022.

Ewe, S. M. L., Gaiser, E. E., Childers, D. L., Iwaniec, D., Rivera-Monroy, V. H., & Twilley, R. R. (2006). Spatial and temporal patterns of aboveground net primary productivity (ANPP) along two freshwater-estuarine transects in the Florida Coastal Everglades. *Hydrobiologia*, *569*(1), 459–474. https://doi.org/10/btmst7

Fitzpatrick, C., Jankowski, K. L., & Reed, D. (2021). *2023 Coastal Master Plan: Attachment B3: Determining Subsidence Rates for Use in Predictive Modeling. Version 3.* Coastal Protection and Restoration Authority.

Friess, D. A., Howard, J., Huxham, M., Macreadie, P. I., & Ross, F. (2022). Capitalizing on the global financial interest in blue carbon. *PLOS Climate*, *1*(8), e0000061. https://doi.org/10/grk7j2

Fujita, Y., Witte, J.-P. M., & van Bodegom, P. M. (2014). Incorporating microbial ecology concepts into global soil mineralization models to improve predictions of carbon and nitrogen fluxes. *Global Biogeochemical Cycles*, *28*(3), 223–238. https://doi.org/10/gn5492

Griscom, B. W., Adams, J., Ellis, P. W., Houghton, R. A., Lomax, G., Miteva, D. A., Schlesinger, W. H., Shoch, D., Siikamäki, J. V., Smith, P., Woodbury, P., Zganjar, C., Blackman, A., Campari, J., Conant, R. T., Delgado, C., Elias, P., Gopalakrishna, T., Hamsik, M. R., … Fargione, J. (2017). Natural climate solutions. *Proceedings of the National Academy of Sciences*, *114*(44), 11645–11650. https://doi.org/10.1073/pnas.1710465114

Hanson, R. S., & Hanson, T. E. (1996). Methanotrophic bacteria. *MICROBIOL. REV.*, *60*, 33. https://doi.org/10/gqt6pg

Harris, J. M., Broussard, W. P., & Nelson, J. A. (2024). Evaluating Coastal Wetland Restoration Using Drones and High-Resolution Imagery. *Estuaries and Coasts*, *47*(6), 1359–1375. https://doi.org/10/g8vgwt

Herbert, E. R., Windham-Myers, L., & Kirwan, M. L. (2021). Sea-level rise enhances carbon accumulation in United States tidal wetlands. *One Earth*, *4*(3), 425–433. https://doi.org/10/gjjpmf

Hillmann, E. R., Rivera-Monroy, V. H., Nyman, J. A., & La Peyre, M. K. (2020). Estuarine submerged aquatic vegetation habitat provides organic carbon storage across a shifting landscape. *Science of The Total Environment*, *717*, 137217. https://doi.org/10.1016/j.scitotenv.2020.137217

Hopkinson, C. S., Morris, J. T., Fagherazzi, S., Wollheim, W. M., & Raymond, P. A. (2018). Lateral Marsh Edge Erosion as a Source of Sediments for Vertical Marsh Accretion. *Journal of Geophysical Research: Biogeosciences*, *123*(8), 2444–2465. https://doi.org/10/gfdp63

Johnson, D., & Geldner, N. (2020). *2023 Coastal Master Plan: Attachment B4: Storm Selection for the ICM. Version 3.* Coastal Protection and Restoration Authority.

Kelleway, J. J., Saintilan, N., Macreadie, P. I., Baldock, J. A., & Ralph, P. J. (2017). Sediment and carbon deposition vary among vegetation assemblages in a coastal salt marsh. *Biogeosciences*, *14*(16), 3763–3779. https://doi.org/10/gcc4w3

Kirwan, M. L., Temmerman, S., Skeehan, E. E., Guntenspergen, G. R., & Fagherazzi, S. (2016). Overestimation of marsh vulnerability to sea level rise. *Nature Climate Change*, *6*(3), 253–260. https://doi.org/10/gc3f6b

Krauss, K. W., Noe, G. B., Duberstein, J. A., Conner, W. H., Stagg, C. L., Cormier, N., Jones, M. C., Bernhardt, C. E., Lockaby, B. G., From, A. S., Doyle, T. W., Day, R. H., Ensign, S. H., Pierfelice, K. N., Hupp, C. R., Chow, A. T., & Whitbeck, J. L. (2018). The role of the upper tidal estuary in wetland blue carbon storage and flux. *Global Biogeochemical Cycles*, *32*(5), 817–839. https://doi.org/10/gdjx6h

Kristensen, E., Bouillon, S., Dittmar, T., & Marchand, C. (2008). Organic carbon dynamics in mangrove ecosystems: A review. *Aquatic Botany*, *89*(2), 201–219. https://doi.org/10/bcsrpq

LaRocque, A., Phiri, C., Leblon, B., Pirotti, F., Connor, K., & Hanson, A. (2020). Wetland Mapping with Landsat 8 OLI, Sentinel-1, ALOS-1 PALSAR, and LiDAR Data in Southern New Brunswick, Canada. *Remote Sensing*, *12*(13), Article 13. https://doi.org/10/gmr9jd

Lawrence, C. R., Neff, J. C., & Schimel, J. P. (2009). Does adding microbial mechanisms of decomposition improve soil organic matter models? A comparison of four models using data from a pulsed rewetting experiment. *Soil Biology and Biochemistry*, *41*(9), 1923–1934. https://doi.org/10/dwjrzn

Lehmann, J., Hansel, C. M., Kaiser, C., Kleber, M., Maher, K., Manzoni, S., Nunan, N., Reichstein, M., Schimel, J. P., Torn, M. S., Wieder, W. R., & Kögel-Knabner, I. (2020). Persistence of soil organic carbon caused by functional complexity. *Nature Geoscience*, *13*(8), Article 8. https://doi.org/10/ghbzzv

Lovelock, C. E., & Reef, R. (2020). Variable Impacts of Climate Change on Blue Carbon. *One Earth*, *3*(2), 195–211. https://doi.org/10/gkcs97

Macreadie, P. I., Anton, A., Raven, J. A., Beaumont, N., Connolly, R. M., Friess, D. A., Kelleway, J. J., Kennedy, H., Kuwae, T., Lavery, P. S., Lovelock, C. E., Smale, D. A., Apostolaki, E. T., Atwood, T. B., Baldock, J., Bianchi, T. S., Chmura, G. L., Eyre, B. D., Fourqurean, J. W., … Duarte, C. M. (2019). The future of blue carbon science. *Nature Communications*, *10*(1), 3998. https://doi.org/10/gh4whz

Macreadie, P. I., Costa, M. D. P., Atwood, T. B., Friess, D. A., Kelleway, J. J., Kennedy, H., Lovelock, C. E., Serrano, O., & Duarte, C. M. (2021). Blue carbon as a natural climate solution. *Nature Reviews Earth & Environment*. https://doi.org/10/gngc3g

Macreadie, P. I., Nielsen, D. A., Kelleway, J. J., Atwood, T. B., Seymour, J. R., Petrou, K., Connolly, R. M., Thomson, A. C., Trevathan-Tackett, S. M., & Ralph, P. J. (2017). Can we manage coastal ecosystems to sequester more blue carbon? *Frontiers in Ecology and the Environment*, *15*(4), 206–213. https://doi.org/10.1002/fee.1484

Macreadie, P. I., Robertson, A. I., Spinks, B., Adams, M. P., Atchison, J. M., Bell-James, J., Bryan, B. A., Chu, L., Filbee-Dexter, K., Drake, L., Duarte, C. M., Friess, D. A., Gonzalez, F., Grafton, R. Q., Helmstedt, K. J., Kaebernick, M., Kelleway, J., Kendrick, G. A., Kennedy, H., … Rogers, K. (2022). Operationalizing marketable blue carbon. *One Earth*, *5*(5), 485–492. https://doi.org/10/grhfg5

Maxwell, T. L., Spalding, M. D., Friess, D. A., Murray, N. J., Rogers, K., Rovai, A. S., Smart, L. S., Weilguny, L., Adame, M. F., Adams, J. B., Austin, W. E. N., Copertino, M. S., Cott, G. M., Duarte de Paula Costa, M., Holmquist, J. R., Ladd, C. J. T., Lovelock, C. E., Ludwig, M., Moritsch, M. M., … Worthington, T. A. (2024). Soil carbon in the world's tidal marshes. *Nature Communications*, *15*(1), 10265. https://doi.org/10/g8t45z

McGuire, K. L., & Treseder, K. K. (2010). Microbial communities and their relevance for ecosystem models: Decomposition as a case study. *Soil Biology and Biochemistry*, *42*(4), 529–535. https://doi.org/10/bxpgk9

Mcleod, E., Chmura, G. L., Bouillon, S., Salm, R., Björk, M., Duarte, C. M., Lovelock, C. E., Schlesinger, W. H., & Silliman, B. R. (2011). A blueprint for blue carbon: Toward an improved understanding of the role of vegetated coastal habitats in sequestering CO_2. *Frontiers in Ecology and the Environment*, *9*(10), 552–560. https://doi.org/10/c9p7gr

McTigue, N. D., Walker, Q. A., & Currin, C. A. (2021). Refining estimates of greenhouse gas emissions from salt marsh "blue carbon" erosion and decomposition. *Frontiers in Marine Science*, *8*. https://doi.org/10/grpfq3

Melillo, J. M., Aber, J. D., Linkins, A. E., Ricca, A., Fry, B., & Nadelhoffer, K. J. (1989). Carbon and nitrogen dynamics along the decay continuum: Plant litter to soil organic matter. *Plant and Soil*, *115*(2), 189–198. https://doi.org/10/bfk5hf

Meselhe, E. A., McCorquodale, J. A., Shelden, J., Dortch, M., Brown, T. S., Elkan, P., Rodrigue, M. D., Schindler, J. K., & Wang, Z. (2013). Ecohydrology component of Louisiana's 2012 Coastal Master Plan: Mass-Balance Compartment Model. *Journal of Coastal Research*, *67*, 16–28. https://doi.org/10.2112/SI_67_2.1

Meselhe, E. A., White, E. D., & Reed, D. J. (2017). *2012 Coastal Master Plan: Appendix C: Modeling Chapter 2 – Future Scenarios* (Louisiana's Comprehensive Master Plan for a Sustainable Coast, p. 32) [Version Final]. The Water Institute of the Gulf. Prepared for the Coastal Protection and Restoration Authority. http://coastal.la.gov/our-plan/2017-coastal-master-plan/

Meselhe, E. A., White, E. D., Wang, Y., & Reed, D. J. (2021). Uncertainty analysis for landscape models used for coastal planning. *Estuarine, Coastal and Shelf Science*, *256*, 107371. https://doi.org/10/gjw9br

Meyer, K. M., Morris, A. H., Webster, K., Klein, A. M., Kroeger, M. E., Meredith, L. K., Brændholt, A., Nakamura, F., Venturini, A., Fonseca de Souza, L., Shek, K. L., Danielson, R., van Haren, J., Barbosa de Camargo, P., Tsai, S. M., Dini-Andreote, F., de Mauro, J. M. S., Barlow, J., Berenguer, E., … Bohannan, B. J. M. (2020). Belowground Changes to Community Structure Alter Methane-Cycling Dynamics in Amazonia. *Environment International*, *145*, 106131. https://doi.org/10/gn49vr

Mitra, S., Wassmann, R., & Vlek, P. L. G. (2005). An appraisal of global wetland area and its organic carbon stock. *Current Science*, *88*(1), 25–35.

NOAA GFDL. (2013). *Climate Model: Temperature Change (RCP 4.5) - 2006 - 2100*. Science On a Sphere. https://sos.noaa.gov/catalog/datasets/climate-model-temperature-change-rcp-45-2006-2100/

Pendleton, L., Donato, D. C., Murray, B. C., Crooks, S., Jenkins, W. A., Sifleet, S., Craft, C. B., Fourqurean, J. W., Kauffman, J. B., Marbà, N., Megonigal, P., Pidgeon, E., Herr, D., Gordon, D., & Baldera, A. (2012). Estimating global "blue carbon" emissions from conversion and degradation of vegetated coastal ecosystems. *PLoS ONE*, *7*(9), e43542. https://doi.org/10/f36w26

Poffenbarger, H. J., Needelman, B. A., & Megonigal, J. P. (2011). Salinity Influence on Methane Emissions from Tidal Marshes. *Wetlands*, *31*(5), 831–842. https://doi.org/10/cfzwmj

Robinson, J. M., Harrison, P. A., Mavoa, S., & Breed, M. F. (2022). Existing and emerging uses of drones in restoration ecology. *Methods in Ecology and Evolution*, *13*(9), 1899–1911. https://doi.org/10/gqd86g

Rosentreter, J. A., Al-Haj, A. N., Fulweiler, R. W., & Williamson, P. (2021). Methane and nitrous oxide emissions complicate coastal blue carbon assessments. *Global Biogeochemical Cycles*, *35*(2), e2020GB006858. https://doi.org/10.1029/2020GB006858

Rosentreter, J. A., Laruelle, G. G., Bange, H. W., Bianchi, T. S., Busecke, J. J., Cai, W.-J., Eyre, B. D., Forbrich, I., Kwon, E. Y., Maavara, T., & others. (2023). Coastal vegetation and estuaries are collectively a greenhouse gas sink. *Nature Climate Change*, *13*(6), 579–587. https://doi.org/10/gr8746

Rosentreter, J. A., Maher, D. T., Erler, D. V., Murray, R. H., & Eyre, B. D. (2018). Methane emissions partially offset "blue carbon" burial in mangroves. *Science Advances*, *4*(6), eaao4985. https://doi.org/10/gdrv5f

Roth, F., Sun, X., Geibel, M. C., Prytherch, J., Brüchert, V., Bonaglia, S., Broman, E., Nascimento, F., Norkko, A., & Humborg, C. (2022). High spatiotemporal variability of methane concentrations challenges estimates of emissions across vegetated coastal ecosystems. *Global Change Biology*, *28*(14), 4308–4322. https://doi.org/10/gpsd48

Ryan, E., Wild, O., Voulgarakis, A., & Lee, L. (2018). Fast sensitivity analysis methods for computationally expensive models with multi-dimensional output. *Geoscientific Model Development*, *11*(8), 3131–3146. https://doi.org/10/gd3sx8

Saltelli, A., Tarantola, S., & Chan, K. P.-S. (1999). A Quantitative Model-Independent Method for Global Sensitivity Analysis of Model Output. *Technometrics*, *41*(1), 39–56. https://doi.org/10/gfsmx2

Sapkota, Y., & White, J. R. (2019). Marsh Edge Erosion and Associated Carbon Dynamics in Coastal Louisiana: A Proxy for Future Wetland-Dominated Coastlines World-Wide. *Estuarine, Coastal and Shelf Science*, *226*, 106289. https://doi.org/10.1016/j.ecss.2019.106289

Smith, C. J., DeLaune, R. D., & Patrick Jr, W. H. (1983). Carbon dioxide emission and carbon accumulation in coastal wetlands. *Estuarine, Coastal and Shelf Science*, *17*, 21–29. https://doi.org/10/ffk8tt

Spivak, A. C., Sanderman, J., Bowen, J. L., Canuel, E. A., & Hopkinson, C. S. (2019). Global-Change Controls on Soil-Carbon Accumulation and Loss in Coastal Vegetated Ecosystems. *Nature Geoscience*, *12*(9), 685–692. https://doi.org/10/gk7s85

Steinmuller, H. E., Dittmer, K. M., White, J. R., & Chambers, L. G. (2019). Understanding the fate of soil organic matter in submerging coastal wetland soils: A microcosm approach. *Geoderma*, *337*, 1267–1277. https://doi.org/10/grpfn3

Taillardat, P., Thompson, B. S., Garneau, M., Trottier, K., & Friess, D. A. (2020). Climate change mitigation potential of wetlands and the cost-effectiveness of their restoration. *Interface Focus*, *10*(5), 20190129. https://doi.org/10/ghz6nk

Visser, J., & Duke-Sylvester, S. (2017). LaVegMod v2: Modeling coastal vegetation dynamics in response to proposed coastal restoration and protection projects in Louisiana, USA. *Sustainability*, *9*(9), 1625. https://doi.org/10.3390/su9091625

Wang, H., Piazza, S., Sharp, L., Stagg, C., Couvillion, B., Steyer, G., & McGinnis, T. (2017). Determining the spatial variability of wetland soil bulk density, organic matter, and the conversion factor between organic matter and organic carbon across coastal Louisiana, U.S.A. *Journal of Coastal Research*, *33*. https://doi.org/10.2112/JCOASTRES-D-16-00014.1

Warnell, K., Olander, L., & Currin, C. (2022). Sea level rise drives carbon and habitat loss in the U.S. mid-Atlantic coastal zone. *PLOS Climate*, *1*(6), e0000044. https://doi.org/10/gqddg7

Weston, N. B., Neubauer, S. C., Velinsky, D. J., & Vile, M. A. (2014). Net ecosystem carbon exchange and the greenhouse gas balance of tidal marshes along an estuarine salinity gradient. *Biogeochemistry*, *120*(1–3), 163–189. https://doi.org/10/grpfmw

White, E. D., Bregman, M. C., Dalyander, P. S., Foster-Martinez, M., Georgiou, I. Y., Hanegan, K., Lindquist, D., Miner, M. D., Reed, D. J., Visser, J. M., Wang, Y., & WANG, Z. (2023). *2023 Coastal Master Plan: Attachment C2: 50-Year FWOA Model Output, Regional Summaries—ICM. Version 3.* (p. 194). Coastal Protection and Restoration Authority.

White, E. D., Meselhe, E., McCorquodale, A., Couvillion, B., Dong, Z., Duke-Sylvester, S., & Wang, Y. (2017). *2017 Coastal Master Plan: Attachment C3-22 – Integrated Compartment Model (ICM) Development* (Attachment Nos. C3-22; 2017 Coastal Master Plan).

Wieder, W. R., Allison, S. D., Davidson, E. A., Georgiou, K., Hararuk, O., He, Y., Hopkins, F., Luo, Y., Smith, M. J., Sulman, B., Todd-Brown, K., Wang, Y.-P., Xia, J., & Xu, X. (2015). Explicitly representing soil microbial processes in Earth system models. *Global Biogeochemical Cycles*, *29*(10), 1782–1800. https://doi.org/10/ghm2dn

Wieder, W. R., Bonan, G. B., & Allison, S. D. (2013). Global soil carbon projections are improved by modelling microbial processes. *Nature Climate Change*, *3*(10), Article 10. https://doi.org/10/gghjzf

Wieder, W. R., Grandy, A. S., Kallenbach, C. M., Taylor, P. G., & Bonan, G. B. (2015). *Representing life in the Earth system with soil microbial functional traits in the MIMICS model* [Preprint]. Biogeosciences. https://doi.org/10.5194/gmdd-8-2011-2015

Williamson, P., & Gattuso, J.-P. (2022). Carbon Removal Using Coastal Blue Carbon Ecosystems Is Uncertain and Unreliable, With Questionable Climatic Cost-Effectiveness. *Frontiers in Climate*, *4*, 853666. https://doi.org/10/grnn2p

Wylie, L., Sutton-Grier, A. E., & Moore, A. (2016). Keys to successful blue carbon projects: Lessons learned from global case studies. *Marine Policy*, *65*, 76–84. https://doi.org/10/gjrdc9

Zhang, X., Xiao, X., Qiu, S., Xu, X., Wang, X., Chang, Q., Wu, J., & Li, B. (2022). Quantifying latitudinal variation in land surface phenology of *Spartina alterniflora* saltmarshes across coastal wetlands in China by Landsat 7/8 and Sentinel-2 images. *Remote Sensing of Environment*, *269*, 112810. https://doi.org/10/gnk7vm